Structural, thermodynamic, electronic and mechanical properties of MCO$_3$ (M: Ca, Fe) precursor materials for Li-ion batteries

M T Morukuladi[1], N L Lethole[1], M C Masedi[1], N N Ngoepe[1] and P E Ngoepe[1]
[1]Materials Modelling Centre, University of Limpopo, Private Bag x1106, Sovenga, 0727, South Africa

Email address: tebogo.morukuladi@ul.ac.za

Abstract. First principle calculations were carried out on the structural, thermodynamic, electronic and mechanical properties of MCO$_3$ precursor materials at 0K to investigate their possible application as cathodes in Li-ion batteries. Li-ion batteries are the most crucial power sources for portable electronic devices. However, their performance greatly depends on the cathode materials, which serves as a host structure for Li ions. In this study we have performed DFT+U calculations using the plane-wave pseudopotential method framed within Perdew Burke Ernzerhof general gradient approximation (PBE-GGA) approach as embedded in the VASP code. The structural lattice parameters were calculated to 95% agreement with the experimental data, ensuring robustness of the approach employed. The calculated heats of formation are relatively low, suggesting thermodynamic stability. The electronic density of states showed that CaCO$_3$ is an insulator whereas FeCO$_3$ is predicted to be metallic, suggesting good electric conductivity on the latter.

1. Introduction

Lithium ion batteries have been widely investigated in the last decades for their application in energy storage due to their excellent cathode materials [1]. Li-ion batteries have different available cathode materials such as lithium iron phosphate, lithium cobalt oxide, lithium manganese oxide etc. Amongst all these cathode materials, lithium cobalt oxide (LiCoO$_2$) was reported as a better cathode material as compared to other cathode materials due to the high energy density translating into a long run-time for portable devices such as cell phones, tablets, laptops and cameras [2]. However, it was later reported that the very same LiCoO$_2$ cathode material was expensive and toxic [3]. As such, various transition metals were largely investigated alternative to the current widely used cathode materials. These include lithium and manganese rich composite Li$_{1+x}$M$_{1-x}$O$_2$ which are known for their high capacity (>200mAh/g) and improved structural stability [4]. However, the electrochemical performance of Li$_{1+x}$M$_{1-x}$O$_2$ compound depends on physical properties of the precursor materials which serve as a source of lithium. Hence, in this work we performed preliminary studies on the transition metal carbonate precursor materials namely calcium carbonate (CaCO$_3$) and iron carbonate (FeCO$_3$), to investigate their potential application as cathode materials in Li-Ion batteries. We have calculated their equilibrium cell parameters, heats of formations, elastic constants, band structures and densities of states to mimic stabilities at 0K. In Figure 1 we present the schematic atomic arrangement in the MCO$_3$ crystal system. MCO$_3$ compound crystallises in the R3cH space group. The transition metal atoms occupy the octahedral positions whilst the carbon atoms are in tetrahedral coordination with oxygen atoms.
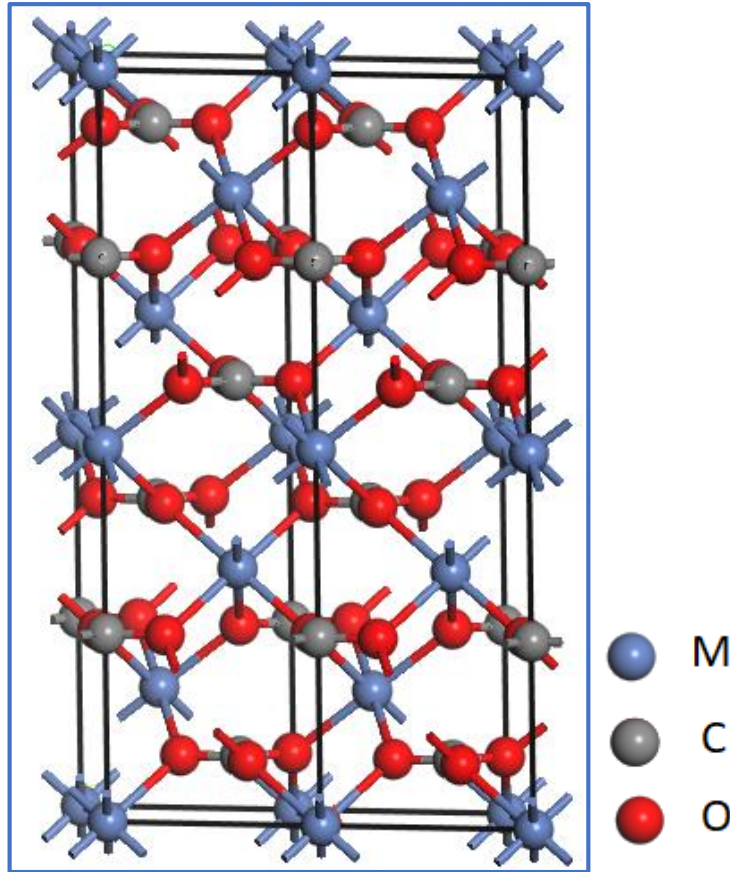
Figure 1. Schematic representation of atomic arrangements in MCO₃ system.

2. Computational Methodology

The first principle calculations based on the pseudopotential plane-wave within density functional theory (DFT) were performed using the Vienna *ab-initio* Simulation Package (VASP) code [5]. The ultrasoft pseudopotential was adopted to simulate the ion-electron interaction [6]. The generalised gradient approximation (GGA) with Hubbard parameter (U) [7] within the Perdew-Burke-Ernzerhof (PBE) functional [8, 9] was utilised to model the exchange-correlation. The plane-wave cut-off energy of 500 eV and Monkhorst and Pack k-points [10] mesh parameter of 4x4x4 were sufficient to converge the total energy of MCO₃ system to within 0.01 eV. Structure optimisation was first performed on the ionic positions and the unit cell size using GGA-PBE exchange correlation, followed by self-consistent calculations of heats of formation, density of states (DOS), band structure and elastic constants with a fixed unit cell volume.

3. Results and Discussions

3.1. Structural, Thermodynamic and Mechanical Properties

In Table 1 we show the DFT+U calculated equilibrium cell parameters, heats of formation, elastic constants and Pugh ratio (B/G) for MCO₃ systems. The available experimental data is also given. The equilibrium cell parameters were obtained by performing full geometry optimisations of atomic positions. The calculated cell parameters for CaCO₃ and FeCO₃ were found to be in good agreement with the experimental values to within 3.4% and 1.36% respectively. This suggests the quality of the approach employed. The calculated heats of formations for all MCO₃ structures are negative, suggesting thermodynamic stability. However, the experimental heats of formations are not available for comparison hence our results can be used for benchmarking in the future. Moreover, we calculated the elastic properties for CaCO₃ and FeCO₃ to determine their mechanical stability and compressibility. The elastic constants are basic parameters closely related to the hardness of the material, which inherently depends on the bond distance and microstructure. To describe the elastic behaviour of trigonal systems completely, six single-crystal elastic constants $(C_{11}, C_{12}, C_{13}, C_{14}, C_{33}, C_{44})$ [11] are

needed. For trigonal crystal systems to be considered mechanically stable, the following Born necessary stability conditions must be satisfied [12].

$$C_{11} - |C_{12}| > 0, (C_{44} + C_{12})C_{33} - 2C_{13}^2 > 0, (C_{11} + C_{12})C_{44} - 2C_{14}^2 > 0 \quad (1)$$

We note that the necessary stability condition for $CaCO_3$ are satisfied, indicating mechanical stability. On the other hand, the stability conditions for $FeCO_3$, in particular $(C_{44} + C_{12})C_{33} - 2C_{13}^2 > 0$ and $(C_{11} + C_{12})C_{44} - 2C_{14}^2 > 0$ are not satisfied, suggesting mechanical instability. Furthermore, the bulk (B), shear (G) and Young's (E) moduli were calculated using the Voigt-Ruess-Hill approximation method from the obtained elastic constants. The bulk (B) modulus determines the hardness of materials, shear (G) modulus describes the response of materials to deformation and Young modulus (E) determine stiffness of materials. In order to determine the brittleness and ductility of MCO_3 materials, we have calculated the B/G ratio proposed by Pugh [13]. Materials are considered ductile if the Pugh's value is greater than 1.75, and brittle if less than 1.75. We note that our calculated B/G ratio is less than 1.75, suggesting brittleness (i.e. structural deformation after bending).

Table 1. Calculated and experimental lattice parameters, heats of formations, elastic constants and Pugh ratio for MCO_3 system.

	$CaCO_3$	Experimental [14]	$FeCO_3$	Experimental [15]
a (Å)	5.162	4.989	4.732	4.668
c (Å)	17.711	17.044	15.207	15.372
V (Å³)	411.322	367.32	294.842	292.570
ΔH_f (kJ/mol)	-1030.902		-583.246	
C_{ij} (GPa)				
C_{11}	125.57		703.63	
C_{12}	40.73		-588.10	
C_{13}	30.07		82.41	
C_{14}	12.03		101.32	
C_{33}	68.06		135.88	
C_{44}	31.44		-152.80	
B	55.05		57.04	
G	33.36		111.44	
E	83.25		190.09	
B/G	1.6402		0.5118	

3.2. Electronic Properties

3.2.1. Density of States. In order to gain knowledge on the electronic properties of $CaCO_3$ and $FeCO_3$, we have calculated their densities of states (DOS) and band structures (BS). In Figure 2 we present the total density of state (TDOS) and partial density of states (PDOS) for $CaCO_3$ and $FeCO_3$. The Fermi level (E_F) is taken as zero energy in total density of state and partial density of state spectra. We observe that the $CaCO_3$ system is characterised by a relatively wide energy band gap of -4.818eV near the Fermi level suggesting insulator behaviour and poor electronic conductivity. On the other hand, $FeCO_3$ shows non energy band gap. Moreover, the Fermi level falls on the spin–down *Fe 3d* band suggesting metallic behaviour and good electronic conductivity. The partial DOS for $CaCO_3$ (Figure 2a) show that the states around Fermi level are predominately *O 2p* with minimum contribution from Ca and C, whereas $FeCO_3$ (Figure 2b) is dominated by *Fe 3d* states.
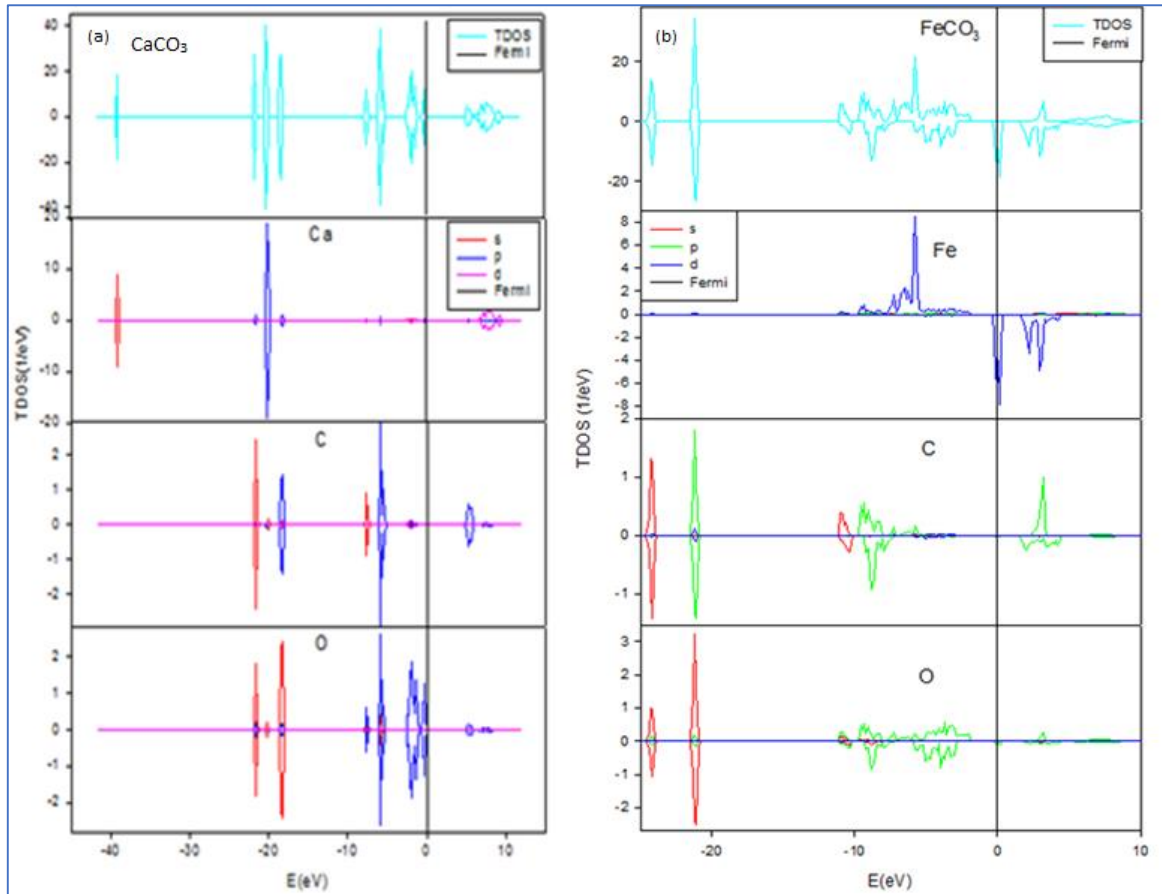
Figure 2. Total and partial DOS for (a) $CaCO_3$ and (b) $FeCO_3$ systems.

3.2.2. Band Structures. The calculations of electronic band structures along the symmetry lines of the Brillouin zone are shown in Figure 3. The band structure plot for $CaCO_3$ (Figure 3a) shows an indirect energy band gap of 4.824eV along high symmetry lines Γ (0,0,0) and L(1/2,1/2,1/2), suggesting that the system is a magnetic insulator. The valence maximum is located near the middle of an edge joining a trigonal face at -0.071eV while the conduction band minimum is located near the centre of the Brillouin zone (Γ) at 4.754eV with respect to the Fermi level. Moreover, band structure plot for $FeCO_3$ (Figure 3b) display no energy band gap at the Fermi level, suggesting a metallic characteristic and good electronic conductivity, the valence band states overlap the Fermi level to the conduction band.
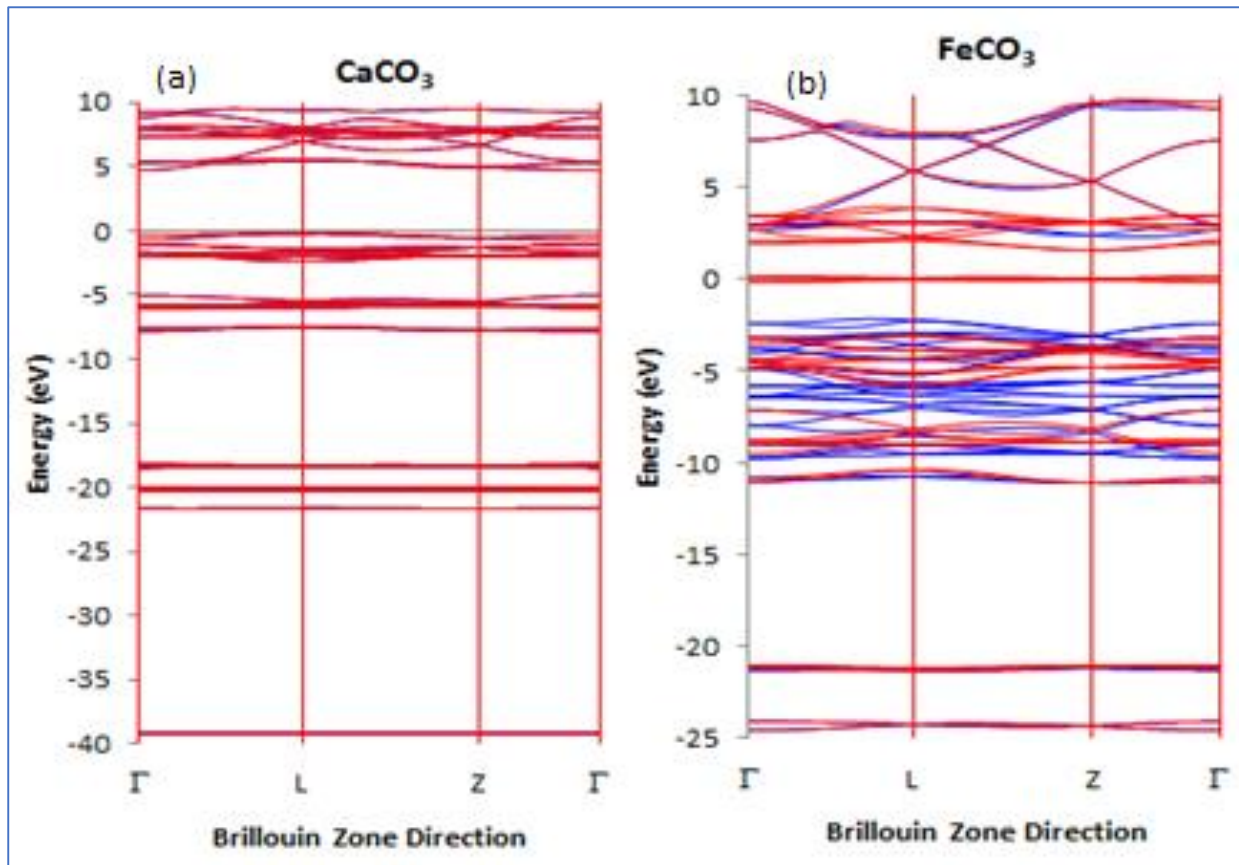
Figure 3. The electronic band structure plots for (a) $CaCO_3$ and (b) $FeCO_3$.

4. Conclusions

The structural, thermodynamic, electronic and mechanical properties of MCO_3 (M: Ca and Fe) compounds have been investigated using the first principle calculations. Structural properties were found to be in good agreement with the experimental data which validate the approach employed. The calculated heats of formation have shown that MCO_3 systems are thermodynamically stable since they have negative values. Moreover, the calculated electronic density of states and band structures predicted that $CaCO_3$ is an insulator whereas $FeCO_3$ is metallic. Lastly, the mechanical properties for MCO_3 compounds showed that $CaCO_3$ satisfy the necessary stability criteria indicating that it is mechanically stable, while on the other hand $FeCO_3$ did not satisfy all the stability criterion for trigonal systems indicating mechanical instability.

5. References

1. Liu K, Liu Y, Lin D, Pei A and Cui Y 2018 Materials for lithium-ion battery safety *Sci. Adv.* **4** 9820.
2. Mizushima K, Jones PC, Wiseman PJ and Goodenough JB 1980 LixCoO2 (0 < x < 1): A new cathode material for batteries of high energy density *Mater. Res.***15** 789.
3. Yoshio M, Brodd RJ and Kozawa A 2009 Lithium ion batteries *J. Sci. Technol.* **46** 299.
4. Lu Z, Macneil DD and Dahn JR 2001 Layered cathode materials Li[NixLi(1/3.2x/3) Mn(3/3.x/3)] O_2 for lithium ion batteries *Electrochem. Solid-State Lett* **4** 194.
5. Kresse G, Marsman M and Furthmuller J 2018 Computational materials physics *Fac. Phys.* **12** 1090.
6. Vanderbilt D 1990 Soft self-consistent pseudopotentials in a generalized eigenvalue formalism *Phys. Rev. B* **41** 7895.

7. Kulik J 2015 Perspective: treating electron over-delocalization with the DFT + U method, *J. Chem. Phys.* **142** 240901.
8. Perdew JP and Wang Y 1992 Accurate and simple analytic representation of the electron-gas correlation energy *Phys. Rev. B* **45** 13244.
9. Perdew JP, Burke K and Ernzerhof M 1996 Generalized gradient approximation made Simple Phys. *Rev. Lett* **77** 3865.
10. Monkhorst HJ and Pack JD 1976 Special points for brillouin-zone integrations *Phys. Rev. B* **13** 5188.
11. Chinh PD 2007 Estimates for the elastic moduli of random trigonal polycrystals and their macroscopic uncertainty *Int. J. Solid-Struct.* **44** 2772.
12. Mei Y, Pang D and Cheng N 2018 Electronic and mechanical properties of trigonal boron nitride by first-principles calculations *Physica E Low Dimens. Syst. Nanostruct.* **101** 385.
13. Pugh SF 1954 Relations between the elastic moduli and the plastic properties of polycrystalline pure metal J. Sci. **45** 843.
14. Zhang J and Reeder RJ 1999 Comparative compressibilities of calcite-structure carbonates: deviations from empirical relations Am. Mineral.**84** 870.
15. Navrotsky A and Chai L 1993 Thermochemistry of carbonate-pyroxene equilibria," contributions to mineralogy and petrology *Cont. Mineral. Petro.* **114** 147.